Phosphorylation of c-Abl by Protein Kinase Pak2 Regulates Differential Binding of ABI2 and CRK†

Jin-Hun Jung,‡ Ann Marie Pendergast,§ Patricia A. Zipfel,‖,⊥ and Jolinda A. Traugh*,‡

Department of Biochemistry, University of California, Riverside, California 92521, Department of Pharmacology and Cancer Biology, and Department of Surgery, Duke University Medical Center, Durham, North Carolina 27710, and Department of Surgery, Durham VA Medical Center, Durham, North Carolina 27705

Received August 1, 2007; Revised Manuscript Received November 5, 2007

ABSTRACT: The tyrosine kinase c-Abl is implicated in a variety of cellular processes that are tightly regulated by c-Abl kinase activity and/or by interactions between c-Abl and other signaling molecules. The interaction of c-Abl with the Abl interactor protein Abi2 is shown to be negatively regulated by phosphorylation of serines 637 and 638. These serines are adjacent to the PxxP motif (PTPPKRS^{637}S^{638}SFR) that binds the SH3 domain of Abi. Phosphorylation of the Abl 593−730 fragment by Pak2 dramatically reduces Abi2 binding (∼90%). Mutation of serines 637−639 to alanine (3A) or aspartate (3D) results in an increased tyrosine kinase activity of c-Abl 3D, and a slight reduction of the activity of the 3A mutant, as compared to wild-type (WT) c-Abl. The interaction between Abi2 and c-Abl 3D is inhibited by 80%, as compared to WT c-Abl or c-Abl 3A. This is accompanied by a 2-fold increase in binding of Crk to c-Abl 3D. The data indicate a molecular mechanism whereby phosphorylation of c-Abl by Pak2 inhibits the interaction between the SH3 domain of Abi2 and the PxxP motif of c-Abl. This phosphorylation enhances the association of c-Abl with the substrate Crk and increases c-Abl-mediated phosphorylation of Crk, thus altering the association of Crk with other signaling molecules.

The c-Abl nonreceptor tyrosine kinase was first identified as the normal cellular homolog of the v-Abl oncoprotein of the Abelson murine leukemia virus (*1*, *2*). The tyrosine kinase has been implicated in cell growth, reorganization of the cytoskeleton, apoptosis, and stress responses (*3*−*6*). c-Abl is ubiquitously expressed in mammalian tissues and is present at many subcellular sites, including the nucleus, cytoplasm, mitochondria, the endoplasmic reticulum (ER), and the plasma membrane (*7*−*10*). Nuclear c-Abl is activated in response to DNA damage (*11*, *12*). The membrane/cytoskeletal-associated c-Abl is activated by growth factors PDGF and EGF in fibroblasts (*13*). In rat fibroblast cells, the ER-localized c-Abl is translocated to mitochondria by ER stress-inducing agents, which contributes to cytochrome *c* release and apoptosis (*10*). In addition, the treatment of cells with hydrogen peroxide stimulates the activity of the cytoplasmic pool of c-Abl, which is involved in H_2O_2-induced apoptosis (*14*).

Many proteins interact with c-Abl through multiple functional domains, including Src-homology domains 3 and 2 (SH3, SH2) at the N-terminus, followed by the tyrosine kinase domain (Src-homology 1, SH1), and three PxxP motifs at the C-terminus of the SH1 domain (*6*). The Abl interactor proteins Abi1[1] and Abi2 bind c-Abl at both the SH3 domain and the third PxxP motif and are phosphorylated by c-Abl in vitro (*15*−*17*). Abi suppresses the Abl transforming activity, without directly inhibiting the Abl kinase activity. Overexpression of Abi1 greatly reduces the transforming activity of the Abelson leukemia virus expressing p160 v-Abl in NIH-3T3 cells; the SH3 domain of Abi1 is required for inhibition (*16*, *18*). The interaction between the SH3 domain of c-Abl and the PxxP motif of Abi2 is blocked by truncating the N-terminal region (aa 1−157) of Abi2 and removing the PxxP site, resulting in activation of the tyrosine kinase and the transforming properties of c-Abl in NIH-3T3 cells (*15*). The Abi2 protein is downregulated by oncogenic forms of the Abl and Src tyrosine kinases through ubiquitination and proteosome degradation in fibroblasts (*19*). These studies suggest that the c-Abl kinase and the Abi protein may regulating each other, although the molecular mechanism is not clearly understood.

The Crk (*c*hicken tumor virus no. 10 *r*egulator of *k*inase) adaptor protein is one of the most studied substrates for the c-Abl kinase and contains one SH2 domain followed by two SH3 domains. Crk is involved in the formation of signal transduction protein complexes, and identified proteins that interact with Crk include the guanine-nucleotide exchange factor C3G, Crk-associated substrate p130^{CAS} (CAS), paxillin, insulin receptor substrate (IRS) proteins, and c-Abl (*20*−*24*). The N-terminal SH3 domain of Crk interacts with two

† This research was supported by United States Public Health Service Grants GM26738 to J.A.T. and CA70940 to A.M.P.

* Corresponding author. Tel: 951-827-4239. Fax: 951-827-4294. E-mail: jolinda.traugh@ucr.edu.

‡ University of California, Riverside.

§ Department of Pharmacology and Cancer Biology, Duke University Medical Center.

‖ Department of Surgery, Duke University Medical Center.

⊥ Department of Surgery, Durham VA Medical Center.

[1] Abbreviations: Abi, Abl interactor protein; Pak2, p21-activated protein kinase 2; SH, Src-homology domain; PIP_2, phosphatidylinositol-4,5-biphosphate; GST, glutathione S-transferase; HA, hemagglutinin epitope.

10.1021/bi701533j CCC: $40.75
Published on Web 12/28/2007

PxxP motifs in the C-terminal region of c-Abl (*25*−*27*). Deletion or mutation of the Crk binding region in c-Abl significantly reduces tyrosine phosphorylation of Crk; thus, the physical association between Crk and c-Abl kinase is necessary for phosphorylation of Crk (*26*, *28*).

Phosphorylation of c-Abl has been shown to activate the tyrosine protein kinase activity of c-Abl. Brasher and Van Etten (*29*) reported that autophosphorylation of c-Abl stimulates the activity of c-Abl kinase about 18-fold in vitro, and sequential autophosphorylation at Tyr-412 and Tyr-245 contributes to the full catalytic activity. Tyr-412 is located in the activation loop of the Abl kinase domain (SH1) and is phosphorylated by c-Abl or by c-Src (*13*, *30*). The ATM (ataxia telangiectasia-mutated) protein kinase phosphorylates c-Abl at Ser465 in vitro, and activates c-Abl in response to ionizing radiation (*31*). Roig et al. (*32*) have shown that the p21-activated protein kinase Pak2/γ-PAK phosphorylates c-Abl in vitro, and expression of active Pak2 in 293T cells enhances the tyrosine kinase activity of c-Abl. Endogenous c-Abl and Arg are activated upon release from PIP_2-mediated inhibition as a result of PLC-γ1-mediated hydrolysis of PIP_2 or by dephosphorylation by PIP_2-specific phosphatase activity (*33*, *34*).

Pak2 is activated by binding of GTP-bound Cdc42 or by cleavage with caspase 3, followed by autophosphorylation at multiple sites (*35*−*37*). Pak2 is transiently activated in response to a variety of moderate stresses, such as hyperosmolarity, repairable DNA damage, and ionizing radiation, resulting in inhibition of cell growth/division (*38*, *39*). Microinjection of active Pak2 into early frog embryos arrests cell cleavage, while inactive Pak2 has no effect (*40*). Overexpression of wild-type (WT) Pak2 in 293T cells inhibits cell division, whereas kinase-inactive or C-terminal mutants have no effect (*41*). Apoptotic stimuli (anti-Fas, C2 ceramide, tumor necrosis factor, DNA-damaging agents) induce caspase cleavage of Pak2, and activated Pak2 is involved in some of the morphological changes in apoptotic cells (*42*, *43*).

In this study, we specifically examined the role of phosphorylation of c-Abl by Pak2 in the interaction of c-Abl with Abi2 and Crk. The Pak2 phosphorylation sites on c-Abl were identified as serines 637 and 638 in vitro by mass spectrometry, 2D tryptic phosphopeptide mapping, and manual sequencing. The same sites were phosphorylated in 293T cells. GST pull-down assays showed that the interaction of c-Abl with Abi2 was greatly reduced following phosphorylation of c-Abl at these sites. A similar reduction in the association of c-Abl with Abi2 was observed when the serine residues 637−639 were replaced with aspartate (c-Abl 3D), as compared with WT c-Abl and the alanine mutant c-Abl 3A. The tyrosine kinase activity of c-Abl 3D was significantly enhanced as compared to WT, as was the association and phosphorylation of Crk. Thus, phosphorylation of c-Abl by Pak2 stimulates the tyrosine kinase activity of c-Abl by blocking the interaction with Abi2, thus enhancing the association with Crk.

EXPERIMENTAL PROCEDURES

Materials. Cell culture media and reagents were purchased from GIBCO/BRL. Insect cell culture medium EX-CELL 401 was from JRH Biosciences. Superfect reagent was from Qiagene (Chatsworth, CA). Protein A/G agarose, rabbit normal IgG, and rabbit polyclonal anti-Abl antibody (K-12) were purchased from Santa Cruz Biotechnology. Mouse monoclonal anti-Abl antibody (8E9) and horseradish peroxidase-conjugated goat anti-mouse IgG were from PharMingen. Mouse monoclonal anti-Abl antibody (Ab-3) was from Oncogene Sciences. Mouse monoclonal anti-HA antibody (HA.11) was from Covance (Berkeley, CA). Anti-HA antibody-conjugated protein A beads were a gift of Drs. Xuan Liu and Xin Cai, University of California, Riverside. Anti-phosphotyrosine antibody 4G10 was from UBI. [γ-^{32}P]ATP was purchased from NEN. [^{32}P]Orthophosphate was from ICN. The protease inhibitors aprotinin, leupeptin, pepstatin, and phenylmethylsulfonyl fluoride (PMSF) were obtained from Roche. Diphenylcarbamoyl chloride (DPCC)-treated trypsin and bovine serum albumin (BSA) were from Sigma. Factor Xa was purchased from Novagen. Sequence-grade trypsin was purchased from Roche. Cellulose thin-layer chromatography (TLC) sheets were from Selecto Scientific (Suwanee, GA), and silica gel TLC sheets were from EM Science. Glutathione-Sepharose 4B was from Amersham. Bradford assay reagent was from Bio-Rad. The site-directed mutagenesis kit GeneEditor was purchased from Promega. Oligonucleotides were from Sigma Genosis. Polyvinylidene difluoride (PVDF) membrane and Sequelon-AA disks were from Millipore. Phenyl isothiocyanate (PITC) was obtained from Pierce. The bacterial expression plasmid pET21(b) for caspase 3 was generously provided by Drs. G. S. Litwack and E. S. Alnemri, Thomas Jefferson University (Philadelphia, PA). The clone for GST-Cdc42 was kindly provided by Dr. Channing Der, University of North Carolina (Chapel Hill, NC). The clone for Cdc42 L61 was generously provided by Dr. J. S. Gutkind, National Institutes of Health (Bethesda, MD), and was subcloned into pcDNA3.1+ vector (Invitrogen).

Site-Directed Mutagenesis. DNA constructs for two mutant forms of c-Abl (3A and 3D) were generated by site-directed mutagenesis. Plasmid pSRα c-Abl WT (*44*) was used as a template DNA. The 3A primer (5′-CAACCCCTCCCAAACGC**GC**C**GC**C**G**CCTTCCGGGAGATGGAC-3′) was used to replace three serine residues with alanine. The 3D primer (5′-CAACCCCTC-CCAAACGC**GA**C**GA**C**GA**CTTCCGGGAGATGGACG-3′) was used to change the three serines to aspartate. Nucleotides different from wild-type sequence are indicated in boldface type, and the changed codons are underlined. The mutant cDNAs were confirmed by sequencing.

Expression and Purification of Proteins. To obtain GST-Pak2, GST-c-Abl (*45*), and GST-Abl 137−671 K/R (*15*), the proteins were expressed individually in insect cells (TN5B-4) using a baculovirus expression system, as described previously (*35*, *46*). GST-fusion proteins Abl 593−730, Abi2 (Δ1−157), and Crk were expressed individually in *Escherichia coli* strain XL1-Blue using the bacterial expression plasmid DNAs pGEX3X-Abl 593−730, pGEX3X-Abi2 (Δ1−157), and pGEX-Crk, as described elsewhere (*13*, *15*). Proteins were purified by affinity chromatography with glutathione-Sepharose 4B beads as described (*15*).

Phosphorylation of c-Abl by Pak2. To phosphorylate c-Abl by Pak2 in vitro, GST-c-Abl and GST-Pak2 were expressed and purified from insect cells as described above. GST-c-Abl (0.5 μg) was phosphorylated with GST-Pak2 (0.1 μg)

in 45 μL reaction mixtures containing 20 mM Tris-HCl, pH 7.4, 10 mM $MgCl_2$, 30 mM 2-mercaptoethanol, 0.2 mM ATP, and [γ-^{32}P]ATP (specific activity 2000 cpm/pmol). GST-Pak2 was preactivated by binding of Cdc42(GTPγS) or by caspase cleavage, followed by autophosphorylation, as described previously (*35*, *47*). After activation of Pak2, caspase 3 inhibitor DEVD-fmk (1 μM) was added to the caspase-activated Pak2 reaction to prevent cleavage of c-Abl. Incubation was at 30 °C for 20 min and terminated by the addition of SDS-sample buffer. Phosphorylated c-Abl was subjected to SDS−PAGE on an 8% gel and analyzed by PhosphorImaging (Molecular Dynamics). Incorporation of ^{32}P into c-Abl was quantified by ImageQuaNT (Molecular Dynamics) and normalized to the amount of c-Abl protein.

Phosphopeptide Mapping and Phosphoamino Acid Analysis. Full-length GST-c-Abl (2 μg), GST-Abl 137−671 K/R (3 μg), and GST-Abl 593−730 (3 μg) were individually phosphorylated with caspase 3-activated Pak2 (0.3 μg). To enhance identification of serine sites, c-Abl was pre-autophosphorylated with cold ATP for 10 min, then active Pak2 and [γ-^{32}P]ATP were added, and incubation was continued for 20 min. The c-Abl proteins were isolated by SDS−PAGE and extensively digested in the excised gel with DPCC-treated trypsin (*48*). The phosphopeptides were analyzed by two-dimensional phosphopeptide mapping and visualized by PhosphorImaging or autoradiography (*36*). Phosphoamino acid analysis, was carried out as described previously (*36*).

Analysis of Tryptic Phosphopeptides by Mass Spectrometry and Manual Sequencing. Abl 137−671 K/R (4 μg) was incubated with ATP in the presence and absence of caspase 3-activated Pak2. The protein was digested with sequence-grade trypsin (0.2 μg) in 100 μL of NH_4HCO_3, pH 8.0. Tryptic digests were analyzed by matrix-assisted laser desorption ionization-time-of-flight (Maldi-TOF) spectrometry and the phosphorylated peptides were identified. The phosphorylated residues were determined by manual Edman degradation as described previously (*37*, *49*).

Binding Analysis of c-Abl and Abi2 in 293T Cells. To examine the interaction between c-Abl and Abi2, exponentially growing 293T cells were transiently transfected using Superfect reagent as described by the manufacturer, and maintained in Dulbecco's modified Eagle's medium supplemented with 10% fetal bovine serum. The cells (2×10^5/60 mm plate) were cotransfected with 1 μg of pSRα c-Abl WT or the mutants (3A, 3D, and K/R) and 3 μg of pCGN HA-Abi2. The DNA constructs pSRα c-Abl and pCGN HA-Abi2 were described elsewhere (*15*, *44*). At 36−48 h post-transfection, cells were collected and resuspended in lysis buffer containing 20 mM Tris-HCl, pH 7.4, 150 mM NaCl, 5 mM EDTA, 1% Triton X-100, 5 mM DTT, phosphatase inhibitors (50 mM NaF, 1 mM Na_3VO_4, 10 nM Okadaic acid), and protease inhibitors (4 μg/mL aprotinin, 4 μg/mL leupeptin, 10 μg/mL pepstatin, 1 mM PMSF). After 30 min on ice, the lysate was cleared by centrifugation and total protein was measured by the Bradford assay.

The interaction between c-Abl and HA-Abi2 in 293T cells was analyzed by immunoprecipitation and Western blotting as described previously (*32*, *50*). Cell lysate (200 μg) was incubated with 1 μg of Abl antibody K-12 for 1 h at 4 °C, protein A/G agarose beads were added, and the mixture incubated for 2 h more. The proteins were analyzed by SDS−PAGE on an 8% gel. c-Abl was detected by Western blotting with Abl antibody 8E9 (*50*), and the membrane was reprobed with HA antibody to detect HA-tagged Abi2 associated with c-Abl. Alternatively, the lysates were incubated with 10 μL anti-HA antibody-conjugated protein A beads to immunoprecipitate HA-tagged Abi2. c-Abl coimmunoprecipitated with Abi2 was detected by Western blotting with anti-Abl 8E9, and the membrane was reprobed with anti-HA antibody to detect HA-Abi2.

Labeling of c-Abl with ^{32}P in 293T Cells. To identify the phosphorylation sites of c-Abl in vivo, HEK 293T cells were labeled with radioactive phosphate, as described previously (*51*). The cells were transfected with WT c-Abl (4 μg) or c-Abl 3D, pcDNA3.1+ plasmids encoding HA-tagged Pak2 (4 μg), and a constitutively active mutant of Cdc42 L61 (4 μg). At 36 h post-transfection, the cells were washed with phosphate-free DMEM supplemented with 10% dialyzed fetal bovine serum, and labeled for 6 h in 4 mL of the same medium with 2 mCi of [^{32}P]orthophosphate per 10 cm plate. Following cell lysis, c-Abl was immunoprecipitated with c-Abl antibodies K-12 (0.4 μg) and Ab3 (0.4 μg), analyzed by SDS−PAGE, and subjected to phosphopeptide mapping.

c-Abl Tyrosine Kinase Assay. The tyrosine kinase activity of c-Abl WT, 3A, and 3D expressed in 293T cells was determined with the substrate GST-Crk following immunoprecipitation of c-Abl from 100 μg of cell lysate with K-12 antibody (1 μg) as described previously (*13*, *32*). The immunoprecipitate was divided into two samples; one was for phosphorylation, and the other was for Western blotting. For phosphorylation, the c-Abl immunoprecipitate was incubated with 1 μg of GST-Crk in 30 μL of buffer containing 20 mM Tris-HCl, pH 7.5, 10 mM $MgCl_2$, 1 mM DTT, 50 μM ATP with [γ-^{32}P]ATP (specific activity 2000 cpm/pmol) for 20 min at 30 °C. Phosphorylation of Crk was analyzed by SDS−PAGE and PhosphorImaging, quantified by ImageQuaNT, and normalized to the amount of c-Abl. c-Abl was detected by Western blotting with 8E9 antibody and quantified by densitometric analysis with Eagle Eye (Stratagene).

GST Pull-Down Assay. For the binding assay, the GST-fusion proteins Abl 593−730 and Abi2 (Δ1−157) were expressed and purified from bacterial cells as described above, and Abi2 was cleaved from GST with factor Xa (10 unit/0.5 mL). GST-cAbl (593−730) (3 μg) bound to beads was preincubated with radioactive ATP and inactive or active Pak2 at 30 °C for 20 min, and then incubated with Abi2 (Δ1−157) (2 μg) at 4 °C for 90 min in buffer containing 20 mM HEPES, pH 7.6, 150 mM NaCl, 0.1% Triton X-100, 10% glycerol, 1 mM DTT, 20 mM NaF, 1 mM Na_3VO_4, 1 mM PMSF, 4 μg/mL of aprotinin, 4 μg/mL of leupeptin, and 10 μg/mL of pepstain. The beads were spun down and washed four times with incubation buffer. The samples were analyzed by SDS−PAGE on a 12.5% gel, and the bound Abi protein was visualized by Coomassie staining and autoradiography.

GST-Crk (2 μg) on glutathione beads was incubated with 100 μg of 293T cell lysate from cells transfected with WT c-Abl, 3A, or 3D and HA-Abi2. The amount of c-Abl protein bound to Crk was analyzed by SDS−PAGE and Western blotting with Abl antibody 8E9.

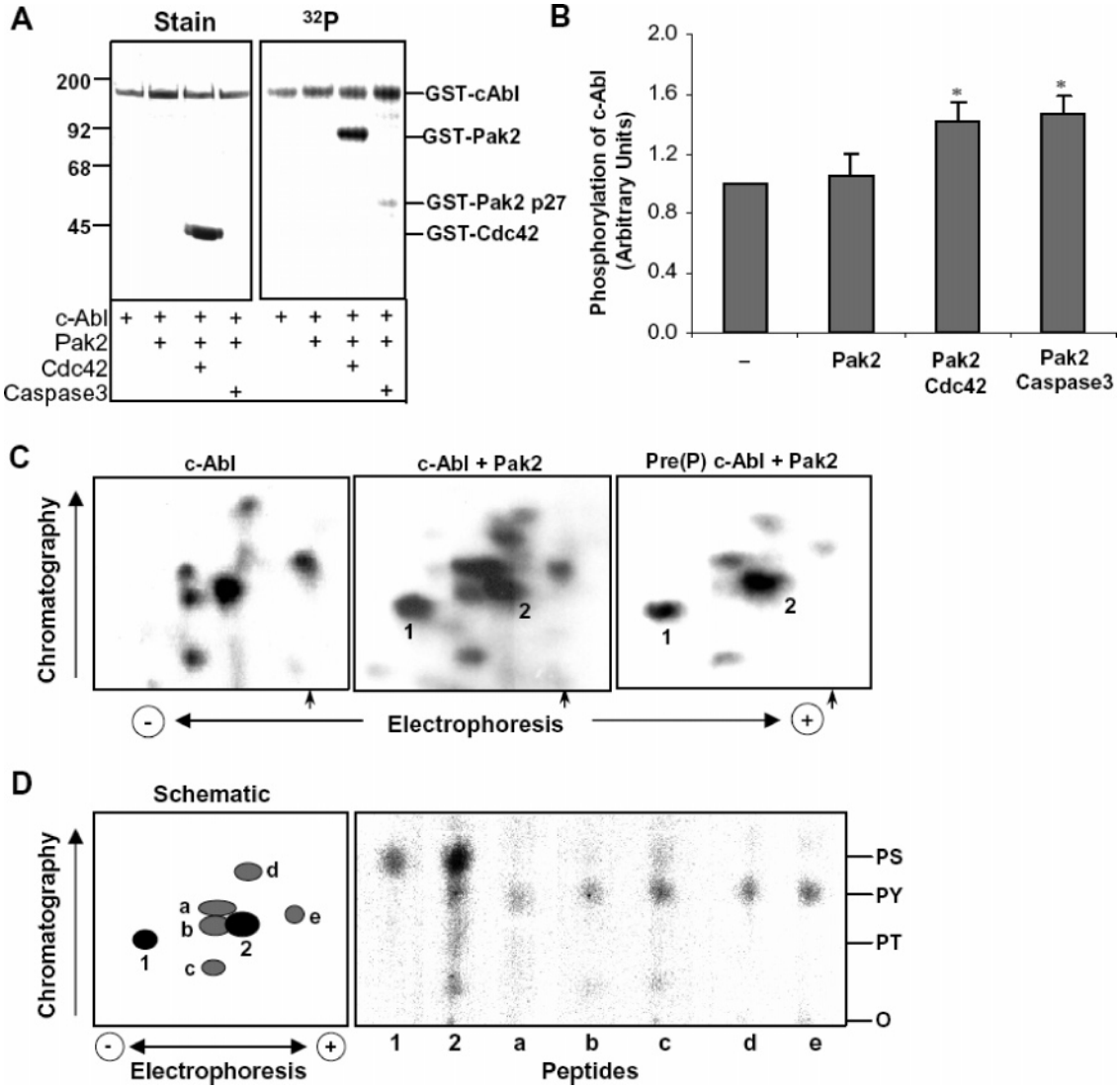

FIGURE 1: Phosphorylation of c-Abl by Pak2. (A) Full-length GST-c-Abl produced in insect cells was incubated with [γ-^{32}P]ATP alone, with nonactivated GST-Pak2, or with GST-Pak2 activated by Cdc42(GTPγS) or by caspase cleavage. Phosphorylation of c-Abl was analyzed by SDS−PAGE and visualized by staining with Coomassie Blue (stain) and by autoradiography (^{32}P). (B) The level of phosphorylation of c-Abl was quantified and normalized to the protein amount. The figure is the mean of three independent experiments, with error bars indicating the standard deviation. The asterisk indicates $p < 0.05$ versus autophosphorylation of c-Abl by unpaired, two-tailed Student *t*-test. (C) c-Abl phosphorylated alone or with Pak2 was analyzed by 2D tryptic phosphopeptide mapping as described in the Experimental Procedures. The autoradiograms are shown. Left panel, c-Abl autophosphorylation; middle panel, c-Abl phosphorylated by caspase-cleaved active Pak2; right panel, c-Abl pre-phosphorylated with ATP and then incubated with active Pak2. The origins are designated by an arrow. The two phosphopeptides produced by Pak2 are labeled 1 and 2. (D) Left panel, the schematic identifies seven phosphopeptides that were subjected to phosphoamino acid analysis. Right panel, the phosphoamino acids are identified by autoradiography. PS, phosphoserine; PY, phosphotyrosine; PT, phosphothreonine; O, origin.

RESULTS

c-Abl is Phosphorylated by Pak2 on Serines 637 and 638 in Vitro. Full length c-Abl, expressed and purified from insect cells as a GST-fusion protein, was incubated alone with [γ-^{32}P]ATP, with nonactivated Pak2, and with Pak2 activated by Cdc42(GTPγS) or by caspase 3 cleavage and analyzed by SDS−PAGE and autoradiography. Significant autophosphorylation on tyrosine was observed with c-Abl alone. In the presence of active Pak2, there was a small increase in the level of phosphorylation of c-Abl (Figure 1A) compared to c-Abl alone, as would be expected due to the high basal level of c-Abl autophosphorylation on multiple sites of tyrosine. Phosphate incorporation on c-Abl was quantified by scintillation counting and normalized to the c-Abl protein. The level of phosphorylation with nonactivated Pak2 was the same as that of autophosphorylated c-Abl. In contrast, a 41% increase in phosphorylation of c-Abl was observed with Cdc42-activated Pak2, and a 46% increase with caspase 3-cleaved Pak2, as compared to c-Abl alone with a *p*-value <0.05 (Figure 1B).

To examine the phosphorylation further, autophosphorylated c-Abl and c-Abl phosphorylated by Pak2 were analyzed by two-dimensional tryptic phosphopeptide mapping via electrophoresis and chromatography and visualized by autoradiography. Six phosphopeptides were identified with c-Abl alone (Figure 1C, left panel). c-Abl phosphorylated by Pak2 had one additional spot and enhanced phosphorylation of a second spot; these were identified as peptides 1

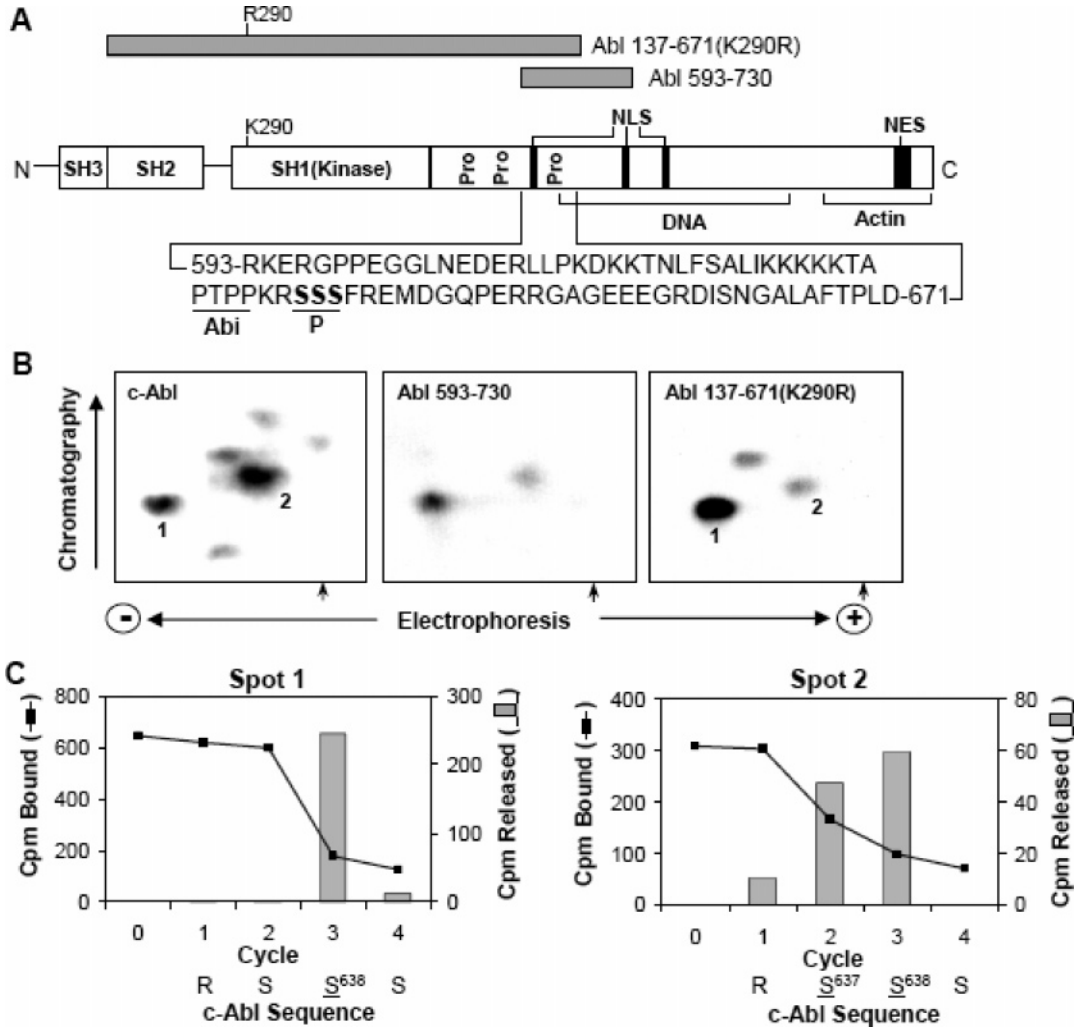

FIGURE 2: Identification of Pak2 phosphorylation sites on c-Abl in vitro. (A) Schematic representation of full length c-Abl, Abl 137−671 (K290R), and Abl 593−730. Identified are Src-homology domains (SH3, SH2, and SH1), three PxxP motifs (Pro), three nuclear localization signals (NLS), a DNA binding domain, an actin binding domain, and a nuclear export signal (NES). The K290R mutation inactivates the SH1 kinase domain. (B) The three forms of c-Abl were phosphorylated by Pak2 and the radiolabeled tryptic phosphopeptides were mapped, as in Figure 1. Left panel, c-Abl prephosphorylated with nonlabeled ATP, then incubated with Pak2 and [γ-^{32}P]ATP; middle panel, Abl 593−730; right panel, Abl 137−671 (K290R). Phosphopeptides 1 and 2 are identified. The origin is indicated by an arrow. (C) Manual sequence analysis of phosphopeptides 1 and 2 of Abl 137−671 (K290R).

and 2 (Figure 1C, middle panel). To enhance the phosphorylation generated by Pak2, c-Abl was autophosphorylated with ATP and then incubated with Pak2 and [γ-^{32}P]ATP. Phosphopeptides 1 and 2 had significantly enhanced phosphorylation, as compared to the c-Abl background autophosphorylation (Figure 1C, right panel). A cartoon (Figure 1D, left panel) is used to identify the phosphopeptides shown in Figure 1C, middle panel. Phosphoamino acid analysis confirmed that peptides 1 and 2 contained phosphoserine, while the other peptides from c-Abl were phosphorylated on tyrosine (Figure 1D, right panel).

Previously, it has been shown that full-length c-Abl and two c-Abl domain proteins, kinase-inactive Abl 137−671-(K290R) and Abl 593−730, were phosphorylated by active Pak2 (*32*). To localize the sites, the three forms of c-Abl were phosphorylated and analyzed by two-dimensional tryptic phosphopeptide mapping. Two major phosphopeptides were observed in all three proteins and identified as peptides 1 and 2 (Figure 2B). In full-length c-Abl, peptide 2 was the major peptide, while peptide 1 was dominant in the Abl fragments. Since spots 1 and 2 were identified in the maps of Abl 137−671(K290R) and Abl 593−730, the two phosphopeptides were localized to amino acids 593−671 (Figure 2A).

To identify which serines were phosphorylated by Pak2, tryptic digests of phosphorylated Abl 137−671(K290R) were analyzed by mass spectrometry. One phosphopeptide was identified, RSSSFR (636−641), which contained a single phosphate (data not shown). To determine which serine was phosphorylated, phosphopeptides 1 and 2 from Abl 137−671(K290R) were subjected to manual sequence analysis. With phosphopeptide 1, there was a single release of ^{32}P at the third cycle. With phosphopeptide 2, ^{32}P was released at the second and third cycle (Figure 2C). Taken together, the data showed that Ser638 was the initial site phosphorylated by Pak2, while there was also significant phosphorylation at Ser637. The two basic amino acids and these serine residues (KRSS) constitute the recognition/phosphorylation sequence previously identified for Pak2 (*52*).

Phosphorylation of Pak2 Sites in 293T Cells. To examine whether the identified sites were phosphorylated in 293T cells overexpressing WT c-Abl, WT Pak2 and constitutively active

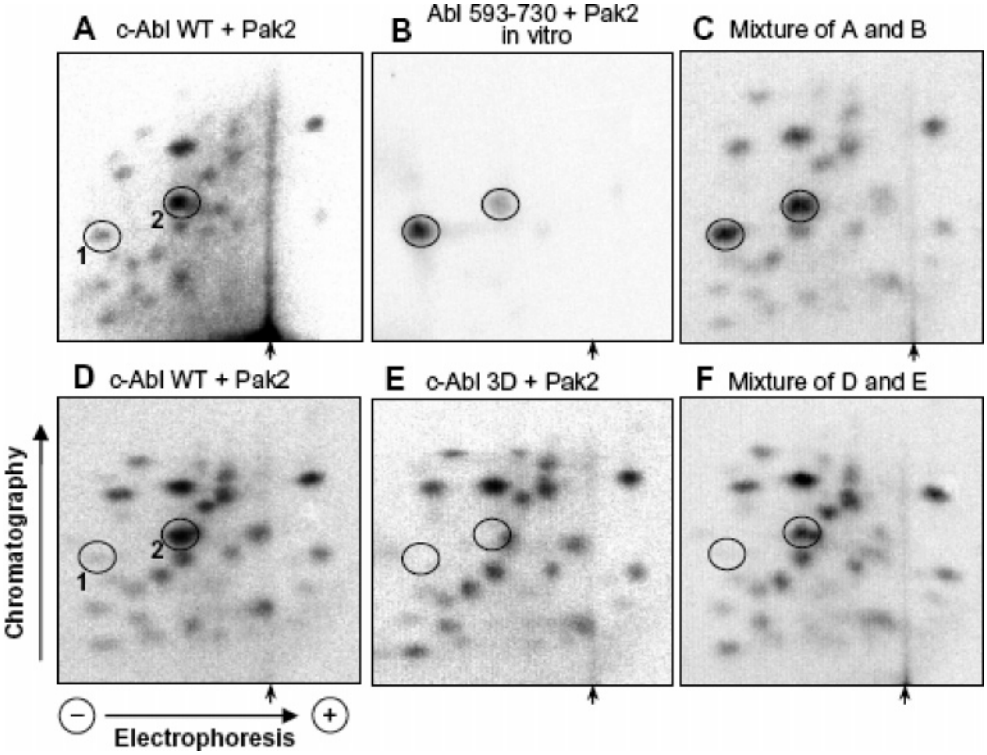

FIGURE 3: Identification of Pak2 phosphorylation sites on c-Abl in 293T cells and in vitro. To identify the Pak2 sites on c-Abl WT or 3D, 293T cells were cotransfected with c-Abl, Pak2, and the active Cdc42 mutant L61 and incubated with [^{32}P]orthophosphate, as described in the Experimental Procedures. c-Abl was immunoprecipitated with c-Abl antibody and subjected to SDS−PAGE, and the phosphopeptides were analyzed by tryptic phosphopeptide mapping and autoradiography. Abl 593−730 phosphorylated by Pak2 in vitro was analyzed in parallel. The origins are indicated by an arrow. The circles depict the positions of peptides 1 and 2 generated by Pak2.

Cdc42 L61, the cells were radiolabeled with [^{32}P]orthophosphate. ^{32}P-labeled c-Abl was immunoprecipitated with c-Abl antibody and subjected to two-dimensional tryptic phosphopeptide mapping. The two phosphopeptides (1 and 2) phosphorylated by Pak2 in vitro (Figure 3B) were also phosphorylated in vivo (Figure 3A and D), and the diphosphorylated peptide was the dominant form. A mixture of peptides from c-Abl phosphorylated in vivo and in vitro comigrated (Figure 3C). To confirm the identity, a site-directed mutant of c-Abl containing three aspartic acid residues in place of serines 637−639 (c-Abl 3D) was subjected to in vivo labeling and tryptic phosphopeptide mapping. The two phosphopeptides were not visible in c-Abl 3D (Figure 3E). The positions of the missing peptides were clearly displayed when the WT and 3D samples were subjected to comigration (Figure 3F).

Phosphorylation of Abl 593−730 by Pak2 Inhibits Binding to Abi2 (Δ1−157). Serines 637−639 are just downstream of the Abl PxxP motif (residues 631−634), which binds to proteins containing SH3 domains such as Abi and Nck (Figure 2A) (*15*, *16*, *26*, *53*). Therefore, we questioned whether Pak2-mediated phosphorylation could alter the interaction between c-Abl and the Abl-interactor protein 2 (Abi2). The binding of Abi2 to c-Abl is mediated by two different sites on Abi2, the N-terminal PxxP motif and the C-terminal SH3 domain (*15*), as indicated in the schematic domain structure of Abi2 (Figure 4A).

To examine the effects of phosphorylation of serine on the binding of Abi2, GST pull-down assays were performed with Abl 593−730 and Abi2 (Δ1−157). GST-Abl 593−730, containing the single C-terminal PxxP motif, was incubated in the presence and absence of nonactivated Pak2 or with Pak2 activated by caspase-cleavage or Cdc42 (GTPγS). Following SDS−PAGE, two bands of phosphorylated Abl were detected in the autoradiogram with active Pak2; the major form migrated at 44 kDa and the minor one at 48 kDa (Figure 4B, top panel). As shown by SDS−PAGE and Coomassie staining, Abi2 (Δ1−157) was associated with nonphosphorylated GST-Abl 593−730 (Figure 4B, lower panel, lanes 2, 3, 5, 6, 8, and 11). Phosphorylation of Abl 593−730 by active Pak2 prevented Abi2 binding (Figure 4B, lanes 4 and 7). The controls showed that caspase 3 did not alter Abi2 bound to Abl 593−730 (Figure 4B, lane 5), and Abi2 was not pulled down with GST or GST-Cdc42 (lanes 1 and 9). Thus, Pak2-mediated phosphorylation of serines 637 and 638 blocked the interaction of Abl with Abi2 in vitro.

Interaction between c-Abl and Abi2 in 293T Cells. To determine whether the association of full length c-Abl and Abi2 was regulated through phosphorylation, we used c-Abl 3D and the alanine mutant (c-Abl 3A), mimicking phosphorylated and nonphosphorylated c-Abl, respectively. WT c-Abl, 3A, 3D and kinase-inactive K/R were individually coexpressed with HA-tagged Abi2 in 293T cells. The level of expression of the mutants 3A, 3D, and K/R was similar, but WT c-Abl was expressed at approximately 20% of the level of the mutants (Figure 5A, top of upper panel). Two forms of HA-Abi2 were detected in the cell lysates containing 3A and 3D, while one form was detected with WT and K/R (Figure 5A, bottom of upper panel). The major form of Abi2 in all of the samples migrated at 59 kDa. A second form of Abi2 migrated at 68 kDa and constituted 5% of the total Abi protein for 3A and 3D. With longer exposure of the Western blot, the upper band of Abi2 was detected with WT,

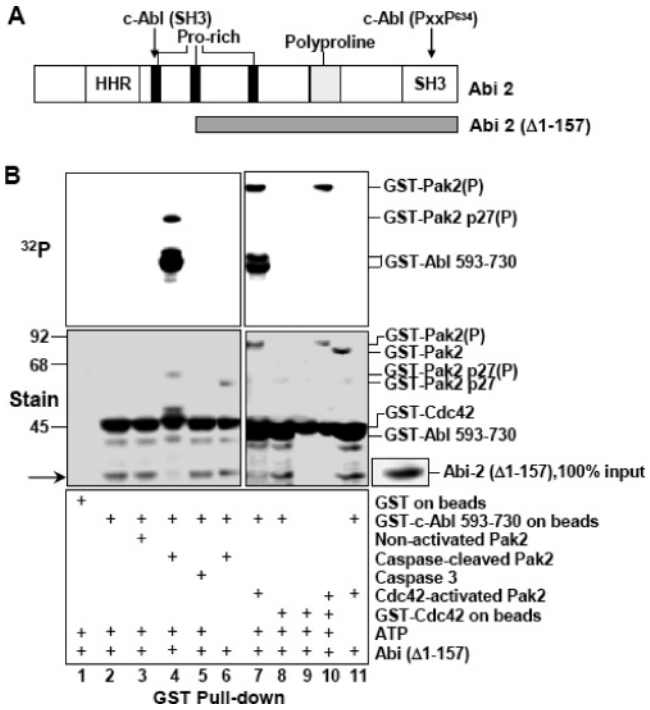

FIGURE 4: Phosphorylation of Abl 593−730 by Pak2 inhibits the binding of Abi2 (Δ1−157). (A) Schematic representation of the Abi2 domain structure and the deletion mutant Abi2 (Δ1−157). Abi2 has a DNA binding region (homeodomain homologous region, HHR), three proline-rich regions, a polyproline stretch, and a SH3 domain at the C-terminus. The binding sites on Abi2 for the SH3 domain and the PxxP[634] motif of c-Abl are indicated by arrows. (B) GST pull-down assay with GST-Abl 593−730 and Abi2 (Δ1−157). Phosphorylation of c-Abl and the effects of phosphorylation by Pak2 on the binding of Abi2 were assayed with nonactivated Pak2 or Pak2 activated by caspase cleavage or by Cdc42(GTPγS), as described in the figure. Abi2 (Δ1−157) was added to the samples and incubation was at 4 °C for 90 min. The phosphoproteins were analyzed by SDS−PAGE and visualized by autoradiography (upper panel) and Coomassie staining (lower panel). The 100% input for Abi2 (Δ1−157) is shown.

but not with the kinase-inactive mutant of c-Abl (data not shown).

The interactions between Abi2 and c-Abl WT and the three mutants were examined following immunoprecipitation with Abl antibody and Western blotting. Similar amounts of c-Abl protein were present in the immunoprecipitates for WT and the mutants (Figure 5A, top of lower panel). Both forms of Abi2 (59 and 68 kDa) were associated with WT c-Abl and 3A (Figure 5A, bottom of lower panel), with a preference for the 68 kDa form. In contrast, the amount of Abi2 associated with 3D was significantly reduced, and the 59 kDa protein was barely visible. With c-Abl K/R, only the 59 kDa protein was present and bound at the same level as the 68 kDa protein bound to c-Abl WT.

The amount of Abi2 bound was normalized to the level of c-Abl, and the amount of 68 kDa bound to the WT was set at 1.0 (Figure 5B). Similar amounts of total Abi2 were associated with c-Abl WT and 3A. The levels of the 68 and 59 kDa proteins were also similar. In contrast, the level of total Abi bound to c-Abl 3D was reduced 5.7-fold. The reciprocal coimmunoprecipitation was performed with anti-HA antibody. c-Abl WT had the highest level of association with HA-Abi2, while 3A and K/R also bound significantly to Abi2 (Figure 5C). In contrast, there was little or no association of c-Abl 3D with HA-Abi2, consistent with the results shown in Figure 5A. Thus, substitution of serines 637−639 with alanine did not have a significant effect on the association of c-Abl with Abi2 as compared to WT c-Abl, but the interaction with Abi2 was drastically reduced with the aspartate mutant. This supports the observation that phosphorylation of c-Abl by Pak2 could downregulate the binding of Abi2.

Tyrosine Kinase Activity of c-Abl WT, 3A, and 3D. The tyrosine kinase activity of c-Abl and the 3A and 3D mutants was analyzed with the substrate Crk. Cells were cotransfected with c-Abl (WT, 3A, or 3D mutant) and HA-Abi2. The expression levels of WT c-Abl and the mutants were the same (Figure 6A, top panel). c-Abl kinase was analyzed by Western blotting with antibodies to c-Abl and phosphotyrosine. The protein levels of WT c-Abl and the mutants were similar, but the extent of endogenous tyrosine phosphorylation in c-Abl 3D was approximately 3-fold higher than that of WT and 3A (Figure 6A, middle panels). When the immunoprecipitates were incubated with Crk and [γ-^{32}P]-ATP, Crk was phosphorylated by WT c-Abl and the mutants. The level of Crk phosphorylation was normalized to the amount of c-Abl protein. WT c-Abl and 3A showed a similar level of autophosphorylation, but the level of autophosphorylation with c-Abl 3D was 1.5-fold higher (Figure 6A, bottom panels). Concomitantly, phosphorylation of Crk by 3A was reduced by 15% as compared to c-Abl WT, while phosphorylation by 3D was increased to 140% of WT and 160% of 3A activity (Figure 6B). Thus, mutation of serines 637−639 to aspartate residues enhanced the autophosphorylation of c-Abl and the subsequent phosphorylation of Crk, as compared to WT and 3A.

Binding of Crk to c-Abl WT and Phosphorylation Site Mutants. Since the physical association of Crk with c-Abl is required for phosphorylation of Crk by c-Abl (*28*, *54*), it was important to examine whether c-Abl 3D altered the binding and phosphorylation of Crk. The 293T cell lysates containing c-Abl WT, 3A, or 3D and HA-Abi2 were used in a GST-pull down analysis with GST-Crk. c-Abl protein was associated with GST-Crk, but not with GST alone (Figure 7, upper panel). In the presence of Abi2, c-Abl WT and 3A bound to Crk to a similar extent, whereas the level of c-Abl 3D associated with Crk was 2-fold higher than that of WT and 3A. This indicated that phosphorylation of c-Abl by Pak2 directly increased the association and phosphorylation of Crk, as compared to nonphosphorylated c-Abl.

DISCUSSION

The serine/threonine kinase Pak2 interacts with and phosphorylates the c-Abl tyrosine kinase, leading to enhanced kinase activity of c-Abl in cells. Using phosphopeptide mapping, mass spectrometry, and manual sequencing analyses, serines 637 and 638 are identified as Pak2 phosphorylation sites in vitro. Phosphopeptide mapping of ^{32}P-labeled c-Abl WT and the mutant c-Abl 3D confirms that the same sites are phosphorylated in 293T cells. These phosphorylation sites are located next to the PxxP motif, which binds the SH3 domain of Abi2 (*15*). Phosphorylation of these sites by Pak2 inhibits the interaction between the Abl PxxP motif and the SH3 domain of Abi2 by up to 90% as compared to nonphosphorylated Abl. Mutation of full-length c-Abl serines

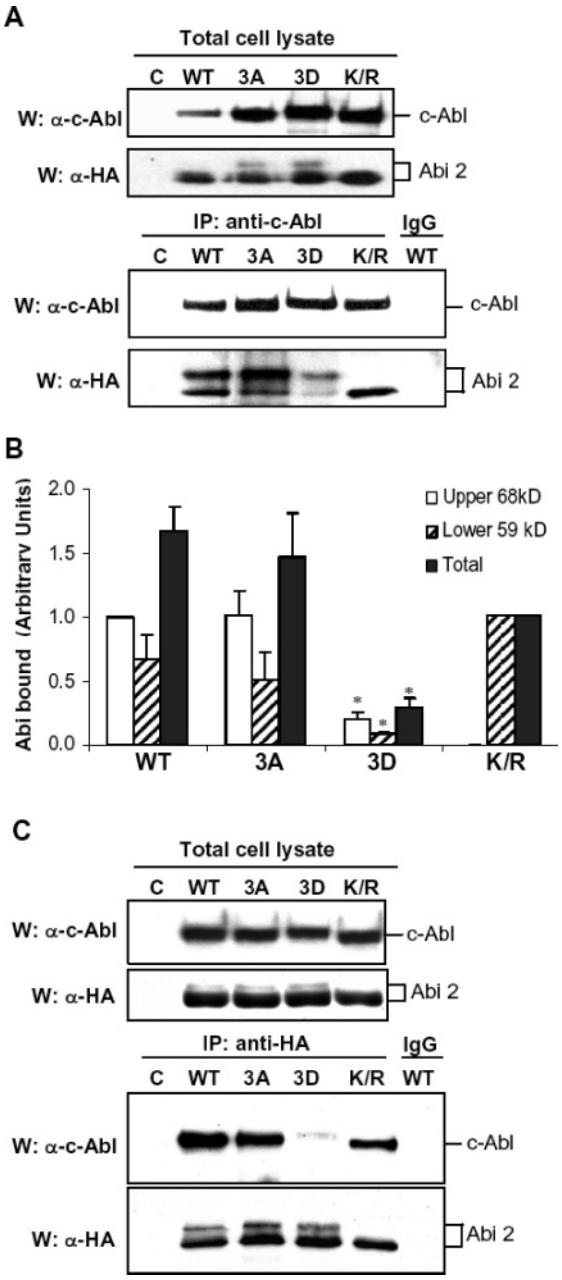

FIGURE 5: Coimmunoprecipitation of c-Abl WT or mutants with Abi2. (A) c-Abl WT, 3A, 3D, and K/R were cotransfected with HA-Abi2 into 293T cells. Total cell lysates were subjected to Western blotting to detect the expression levels of c-Abl and HA-Abi2 with anti-Abl 8E9 and anti-HA antibody, respectively (upper panels). The immunoprecipitates with anti-c-Abl antibody K-12 were analyzed by Western blotting with anti-Abl 8E9. Normal rabbit IgG was used as a control. The same membrane was reprobed with anti-HA antibody to identify HA-tagged Abi2 (lower panels). The blots are representative of three independent experiments. (B) The upper and lower bands of HA-Abi2 and c-Abl in the immunoprecipitates were quantified by Eagle Eye II, and the level of the 68 kDa Abi2 bound to WT c-Abl was set as 1.0. The bar graph illustrates the level of HA-Abi2 bound to WT c-Abl and the mutants and shows the mean of three independent experiments with error bar indicating the standard deviation. The asterisk indicates $p < 0.05$ versus the level of Abi2 bound to WT by unpaired, two-tailed Student *t*-test. (C) Reciprocal coimmunoprecipitation was performed with anti-HA antibody. c-Abl bound to HA-Abi2 was detected by Western blotting with anti-Abl 8E9, and the membrane was reprobed with anti-HA antibody to detect HA-Abi2 (lower panels). Expression levels of c-Abl and Abi2 in cell lysate are shown (upper panels). The blots are representative of three independent experiments.

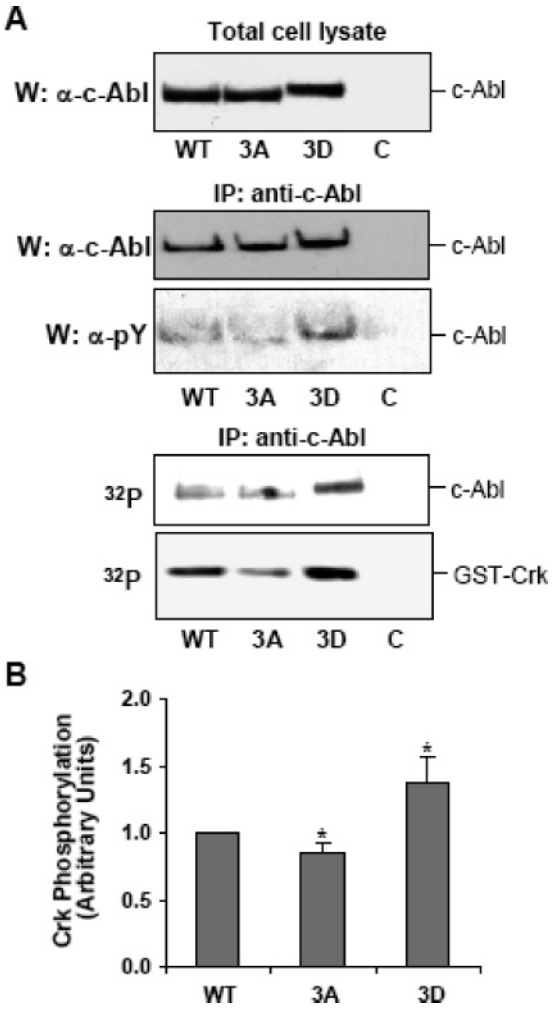

FIGURE 6: Tyrosine kinase activity of c-Abl WT, 3A, and 3D. (A) c-Abl and Abi2 were cotransfected with 293T cells and harvested after 48 h. Expression levels of the WT and mutant forms of c-Abl were detected by Western blotting with c-Abl antibody 8E9 (top panel). Immunoprecipitation with c-Abl antibody K-12 was analyzed by Western blotting with c-Abl antibody 8E9 and anti-phosphotyrosine antibody 4G10 (middle panels). Crk was phosphorylated by immunoprecipitated c-Abl, and ^{32}P incorporation into c-Abl and Crk was visualized by phosphorimaging (lower panels). (B) ^{32}P incorporation into Crk was quantified by ImageQuaNT and normalized to the level of c-Abl protein. The relative tyrosine kinase activity of c-Abl is the average of five independent experiments, with error bars indicating the standard deviation. The asterisk indicates $p < 0.01$ versus WT by unpaired, two-tailed Student *t*-test.

637−639 to aspartate inhibits the association of Abi2 with c-Abl, whereas the alanine mutant does not effect the protein interaction. This inhibition is accompanied by an enhanced c-Abl 3D kinase activity, stimulation of Crk phosphorylation, and a 2-fold increase in Crk binding to c-Abl 3D in the presence of Abi2, as compared to WT c-Abl or the 3A mutant. Thus, Pak2-mediated phosphorylation of c-Abl regulates the interaction of c-Abl with Abi2 and Crk.

The SH3 domains bind PxxP motifs in a left-handed polyproline type II helical conformation, and two opposite orientations are defined by NMR and the X-ray crystalography (*55*, *56*). The type I PxxP motifs have the consensus sequence RxLPP#P (x, any amino acid; #, normally a hydrophobic residue), whereas the type II motifs have Px#PxR. The helix conformation is stabilized predominantly by hydrophobic contacts and additionally by electrostatic

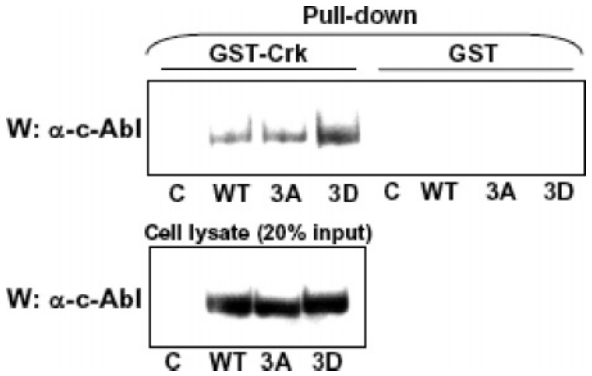

FIGURE 7: Binding of Crk to c-Abl WT, 3A, and 3D in the presence of Abi2. Cells were transfected with c-Abl WT, 3A, or 3D and Abi2. Cell lysate (200 μg) was incubated with 2 μg of GST-Crk or GST (control) on glutathione beads, and the c-Abl immunoprecipitates were analyzed by SDS−PAGE and Western blotting with anti-Abl antibody 8E9 (top panel); c-Abl expression (lower panel).

interactions between the conserved arginine and aspartate or glutamate in the SH3 domain. The Abl region *P*TP*P*-K*R*SSS[639] belongs to the type II motif, and the Pak2 phosphorylation sites Ser637 and Ser638 are adjacent to the conserved arginine. This would allow negative charges introduced by Pak2-dependent phosphorylation to disrupt electrostatic interactions with the conserved arginine, resulting in dissociation of Abi2 from the Abl PxxP motif. In this regard, it has been reported that phosphorylation of Pak1 at Ser21, which is in the binding region for Nck, leads to a reduction in binding of Nck to Pak1 (*57*, *58*).

Abi1/2 appears to antagonize the oncogenic potential of the Abl tyrosine kinases in cells (*15*, *16*). It was initially proposed that association of Abi2 with c-Abl, through binding to both the c-Abl N-terminal SH3 domain and the c-Abl C-terminal PxxP motif, stabilizes the folded (inactive) conformation of the c-Abl kinase (*15*, *59*). Although Abi has not been shown to directly inhibit activation of c-Abl in vitro, disruption of the interaction of c-Abl with Abi results in stimulation of the kinase activity and transforming property of c-Abl in cells (*15*, *16*, *18*). In this regard, our data suggest that phosphorylation-dependent disassociation of Abi2 from c-Abl allows a conformational change in c-Abl, which favors access and association of Crk with two upstream PxxP motifs (PELP[548] and PLLP[592]), leading to phosphorylation by the c-Abl kinase.

Abi2 is a substrate for c-Abl, and the physical interaction between c-Abl and Abi2 is required for phosphorylation of Abi2 (*15*). Treatment with phosphatases confirms that phosphorylation contributes to multiple bands of Abi2, as shown in Western blots of mouse embryo and developing brain lysates (*60*). Consistently, our data show that cells expressing c-Abl and Abi2 have two differently migrating Abi2 proteins. The 68 kDa band is likely due to phosphorylation induced directly or indirectly by c-Abl, as the band appears only in cells expressing c-Abl WT, 3A, and 3D, but not in cells containing kinase-inactive c-Abl (Figure 5A). The phosphotyrosine antibody mainly detects the upper band of Abi2 (data not shown). The 68 kDa form of Abi2 is less than 5% of the total Abi2 in the lysate but displays a significantly higher level of binding to c-Abl than the 59 kDa form, as shown by coimmunoprecipitation. This could be due to an additional interaction between c-Abl and Abi2 through the SH2 domain of c-Abl and tyrosine phosphorylated Abi2. In this regard, Abl has been shown to interact with the Abl substrate, Ras and Rab interactor 1 (Rin1) via the Abl SH3 and SH2 domains, and these interactions stimulate Abl catalytic activity (*61*). Thus, Abl binding to distinct substrates can either activate or inhibit Abl kinase activity.

Phosphorylation of Crk at tyrosine 221 by c-Abl generates the consensus binding site pYxxP (Y[221]AQP) for the SH2 domain of Crk, leading to an intramolecular association between the SH2 domain and phosphotyrosine 221 (*25*, *62*). The resulting intramolecular fold prevents the interaction of Crk with binding partner proteins such as c-Abl, p130 CAS, and C3G (*25*, *63*, *64*). Uncoupling of the Crk-CAS complex by phosphorylation of Crk induces cell death in COS-7 cells (*65*, *66*). Under conditions of moderate stress, Pak2 associates with and phosphorylates c-Abl, stimulating c-Abl tyrosine kinase activity, with the consequent tyrosine phosphorylation and down-regulation of Pak2 (*32*). Under apoptotic conditions, Pak2 is cleaved by caspase 3 and constitutively activated. This would lead to the enhanced phosphorylation of c-Abl and Crk observed in these studies.

ACKNOWLEDGMENT

We thank Drs. Jun Ling, Polygena Tuazon, and Yuan-Hao Hsu, and Barbara Walter for technical advice and support.

REFERENCES

1. Goff, S. P., Gilboa, E., Witte, O. N., and Baltimore, D. (1980) Structure of the abelson murine leukemia virus genome and the homologous cellular gene studies with cloned viral DNA, *Cell 22*, 777−786.
2. Wang, J. Y. J., Ledley, F., Goff, S., Lee, R., Groner, Y., and Baltimore, D. (1984) The mouse c-abl locus molecular cloning and characterization, *Cell 36*, 349−356.
3. Van Etten, R. A. (1999) Cycling, stressed-out and nervous: Cellular functions of c-Abl, *Trends Cell Biol. 9*, 179−186.
4. Wang, J. Y. J. (1999) Integrative signaling through c-Abl: A tyrosine kinase with nuclear and cytoplasmic functions, in *Cancer Drug Discovery and Development* (Gutkind, J. S., Ed.) pp 303−324, Humana Press, Totowa, NJ.
5. Wang, J. Y. J. (2000) Regulation of cell death by the Abl tyrosine kinase, *Oncogene 19*, 5643−5650.
6. Pendergast, A. M. (2002) The Abl family kinases: Mechanisms of regulation and signaling, *Adv. Cancer Res. 85*, 51−100.
7. Van Etten, R. A., Jackson, P., and Baltimore, D. (1989) The mouse type iv c-abl gene product is a nuclear protein and activation of transforming ability is associated with cytoplasmic localization, *Cell 58*, 669−678.
8. Wang, J. Y. J. (1993) Abl tyrosine kinase in signal transduction and cell-cycle regulation, *Curr. Opin. Genet. Dev. 3*, 35−43.
9. Taagepera, S., McDonald, D., Loeb, J. E., Whitaker, L. L., McElroy, A. K., Wang, J. Y. J., and Hope, T. J. (1998) Nuclear-cytoplasmic shuttling of C-ABL tyrosine kinase, *Proc. Natl. Acad. Sci. U.S.A. 95*, 7457−7462.
10. Ito, Y., Pandey, P., Mishra, N., Kumar, S., Narula, N., Kharbanda, S., Saxena, S., and Kufe, D. (2001) Targeting of the c-Abl tyrosine kinase to mitochondria in endoplasmic reticulum stress-induced apoptosis, *Mol. Cell. Biol. 21*, 6233−6242.
11. Kharbanda, S., Ren, R., Pandey, P., Shafman, T. D., Feller, S. M., Weichselbaum, R. R., and Kufe, D. W. (1995) Activation of the c-Abl tyrosine kinase in the stress response to DNA-damaging agents, *Nature 376*, 785−788.
12. Liu, Z.-G., Baskaran, R., Lea-Chou, E. T., Wood, L. D., Chen, Y., Karin, M., and Wang, J. Y. J. (1996) Three distinct signalling responses by murine fibroblasts to genotoxic stress, *Nature 384*, 273−276.
13. Plattner, R., Kadlec, L., DeMali, K. A., Kazlauskas, A., and Pendergast, A. M. (1999) c-Abl is activated by growth factors

and Src family kinases and has a role in the cellular response to PDGF, *Genes Dev. 13*, 2400−2411.
14. Sun, X., Majumder, P., Shioya, H., Wu, F., Kumar, S., Weichselbaum, R., Kharbanda, S., and Kufe, D. (2000) Activation of the cytoplasmic c-Abl tyrosine kinase by reactive oxygen species, *J. Biol. Chem. 275*, 17237−17240.
15. Dai, Z., and Pendergast, A. M. (1995) Abi-2, a novel SH3-containing protein interacts with the c-Abl tyrosine kinase and modulates c-Abl transforming activity, *Genes Dev. 9*, 2569−2582.
16. Shi, Y., Alin, K., and Goff, S. P. (1995) Abl-interactor-1, a novel SH3 protein binding to the carboxy-terminal portion of the Abl protein, suppresses v-abl transforming activity, *Genes Dev. 9*, 2583−2597.
17. Biesova, Z., Piccoli, C., and Wong, W. T. (1997) Isolation and characterization of e3B1, and eps8 binding protein that regulates cell growth, *Oncogene 14*, 233−241.
18. Ikeguchi, A., Yang, H.-Y., Gao, G., and Goff, S. P. (2001) Inhibition of v-Abl transformation in 3T3 cells overexpressing different forms of the Abelson interactor protein Abi-1, *Oncogene 20*, 4926−4934.
19. Dai, Z., Quackenbush, R. C., Courtney, K. D., Grove, M., Cortez, D., Reuther, G. W., and Pendergast, A. M. (1998) Oncogenic Abl and Src tyrosine kinases elicit the ubiquitin-dependent degradation of target proteins through a Ras-independent pathway, *Genes Dev. 12*, 1415−1424.
20. Birge, R. B., Fajardo, J. E., Mayer, B. J., and Hanafusa, H. (1992) Tyrosine-phosphorylated epidermal growth factor receptor and cellular p130 provide high affinity binding substrates to analyze crk phosphotyrosine-dependent interactions in-vitro, *J. Biol. Chem. 267*, 10588−10595.
21. Knudsen, B. S., Feller, S. M., and Hanafusa, H. (1994) Four proline-rich sequences of the guanine-nucleotide exchange Factor C3G Bind with unique specificity to the first Src homology 3 domain of Crk, *J. Biol. Chem. 269*, 32781−32787.
22. Feller, S. M., Ren, R., Hanafusa, H., and Baltimore, D. (1994) SH2 and SH3 domains as molecular adhesives: The interactions of Crk and Abl, *Trends Biochem. Sci. 19*, 453−458.
23. Matsuda, M., Ota, S., Tanimura, R., Nakamura, H., Matuoka, K., Takenawa, T., Nagashima, K., and Kurata, T. (1996) Interaction between the amino-terminal SH3 domain of CRK and its natural target proteins, *J. Biol. Chem. 271*, 14468−14472.
24. Beitner-Johnson, D., Blakesley, V. A., Shen-Orr, Z., Jimenez, M., Stannard, B., Wang, L.-M., Pierce, J., and Leroith, D. (1996) The proto-oncogene product c-Crk associates with insulin receptor substrate-1 and 4PS Modulation by insulin growth factor-I (IGF) and enhanced IGF-I signaling, *J. Biol. Chem. 271*, 9287−9290.
25. Feller, S. M., Knudsen, B., and Hanafusa, H. (1994) C-Abl kinase regulates the protein binding activity of c-Crk, *EMBO J. 13*, 2341−2351.
26. Ren, R., Ye, Z.-S., and Baltimore, D. (1994) Ab1 protein: Tyrosine kinase selects the Crk adapter as a substrate using SH3-binding sites, *Genes Dev. 8*, 783−795.
27. Wang, B., Mysliwiec, T., Feller, S. M., Knudsen, B., Hanafusa, H., and Kruh, G. D. (1996) Proline-rich sequences mediate the interaction of the Arg protein tyrosine kinase with Crk, *Oncogene 13*, 1379−1385.
28. Shishido, T., Akagi, T., Chalmers, A., Maeda, M., Terada, T., Georgescu, M.-M., and Hanafusa, H. (2001) Crk family adaptor proteins trans-activate c-Abl kinase, *Genes Cells 6*, 431−440.
29. Brasher, B. B., and Van Etten, R. A. (2000) c-Abl has high intrinsic tyrosine kinase activity that is stimulated by mutation of the Src homology 3 domain and by autophosphorylation at two distinct regulatory tyrosines, *J. Biol. Chem. 275*, 35631−35637.
30. Dorey, K., Engen, J. R., Kretzschmar, J., Wilm, M., Neubauer, G., Schindler, T., and Superti-Furga, G. (2001) Phosphorylation and structure-based functional studies reveal a positive and a negative role for the activation loop of the c-Abl tyrosine kinase, *Oncogene 20*, 8075−8084.
31. Baskaran, R., Wood, L. D., Whitaker, L. L., Canman, C. E., Morgan, S. E., Xu, Y., Barlow, C., Baltimore, D., Wynshaw-Boris, A., Kastan, M. B., and Wang, J. Y. J. (1997) Ataxia telangiectasia mutant protein activates c-Abl tyrosine kinase in response to ionizing radiation, *Nature 387*, 516−519.
32. Roig, J., Tuazon, P. T., Zipfel, P. A., Pendergast, A. M., and Traugh, J. A. (2000) Functional interaction between c-Abl and the p21-activated protein kinase gamma-PAK, *Proc. Natl. Acad. Sci. U.S.A. 97*, 14346−14351.
33. Plattner, R., Irvin, B. J., Guo, S. L., Blackburn, K., Kazlauskas, A., Abraham, R. T., York, J. D., and Pendergast, A. M. (2003) A new link between the c-Abl tyrosine kinase and phosphoinositide signalling through PLC-gamma 1, *Nat. Cell Biol. 5*, 309−319.
34. Plattner, R., Koleske, A. J., Kazlauskas, A., and Pendergast, A. M. (2004) Bidirectional signaling links the Abelson kinases to the platelet-derived growth factor receptor, *Mol. Cell. Biol. 24*, 2573−2583.
35. Walter, B. N., Huang, Z., Jakobi, R., Tuazon, P. T., Alnemri, E. S., Litwack, G., and Traugh, J. A. (1998) Cleavage and activation of p21-activated protein kinase gamma-PAK by CPP32 (Caspase 3): Effects of autophosphorylation on activity, *J. Biol. Chem. 273*, 28733−28739.
36. Tuazon, P. T., Chinwah, M., and Traugh, J. A. (1998) Autophosphorylation and protein kinase activity of p21-activated protein kinase gamma-PAK are differentially affected by magnesium and manganese, *Biochemistry 37*, 17024−17029.
37. Gatti, A., Huang, Z., Tuazon, P. T., and Traugh, J. A. (1999) Multisite autophosphorylation of p21-activated protein kinase gamma-PAK as a function of activation, *J. Biol. Chem. 274*, 8022−8028.
38. Roig, J., Huang, Z., Lytle, C., and Traugh, J. A. (2000) p21-activated protein kinase gamma-PAK is translocated and activated in response to hyperosmolarity: Implication of Cdc42 and phosphoinositide 3-kinase in a two-step mechanism for gamma-PAK activation, *J. Biol. Chem. 275*, 16933−16940.
39. Roig, J., and Traugh, J. A. (1999) p21-activated protein kinase gamma-PAK is activated by ionizing radiation and other DNA-damaging agents: Similarities and differences to alpha-PAK, *J. Biol. Chem. 274*, 31119−31122.
40. Rooney, R. D., Tuazon, P. T., Meek, W. E., Carroll, E. J., Hagen, J. J., Gump, E. L., Monnig, C. A., Lugo, T., and Traugh, J. A. (1996) Cleavage arrest of early frog embryos by the G protein-activated protein kinase PAK I, *J. Biol. Chem. 271*, 21498−21504.
41. Huang, Z., Ling, J., and Traugh, J. A. (2003) Localization of p21-activated protein kinase gamma-PAK/Pak2 in the endoplasmic reticulum is required for induction of cytostasis, *J. Biol. Chem. 278*, 13101−13109.
42. Lee, N., MacDonald, H., Reinhard, C., Hallenbeck, R., Roulston, A., Shi, T., and Williams, L. T. (1997) Activation of hPAK65 by caspase cleavage induces some of the morphological and biochemical changes of apoptosis, *Proc. Natl. Acad. Sci. U.S.A. 94*, 13642−13647.
43. Jakobi, R., McCarthy, C. C., Koeppel, M. A., and Stringer, D. K. (2003) Caspase-activated PAK-2 is regulated by subcellular targeting and proteasomal degradation, *J. Biol. Chem. 278*, 38675−38685.
44. Pendergast, A. M., Muller, A. J., Havlik, M. H., Clark, R., McCormick, F., and Witte, O. N. (1991) Evidence for regulation of the human abl tyrosine kinase by a cellular inhibitor, *Proc. Natl. Acad. Sci. U.S.A. 88*, 5927−5931.
45. Mayer, B. J., and Baltimore, D. (1994) Mutagenic analysis of the roles of SH2 and SH3 domains in regulation of the Abl tyrosine kinase, *Mol. Cell. Biol. 14*, 2883−2894.
46. Jakobi, R., Huang, Z., Walter, B. N., Tuazon, P. T., and Traugh, J. A. (2000) Substrates enhance autophosphorylation and activation of p21-activated protein kinase gamma-PAK in the absence of activation loop phosphorylation, *Eur. J. Biochem. 267*, 4414−4421.
47. Jakobi, R., Chen, C.-J., Tuazon, P. T., and Traugh, J. A. (1996) Molecular cloning and sequencing of the cytostatic G protein-activated protein kinase PAK I, *J. Biol. Chem. 271*, 6206−6211.
48. Tuazon, P. T., Merrick, W. C., and Traugh, J. A. (1989) Comparative analysis of phosphorylation of translational initiation and elongation factors by seven protein kinases, *J. Biol. Chem. 264*, 2773−2777.
49. Sullivan, S., and Wong, T. W. (1991) A manual sequencing method for identification of phosphorylated amino acids in phosphopeptides, *Anal. Biochem. 197*, 65−68.
50. Pendergast, A. M., Quilliam, L. A., Cripe, L. D., Bassing, C. H., Dai, Z., Li, N., Batzer, A., Rabun, K. M., Der, C. J., Schlessinger, J., and Gishizky, M. L. (1993) BCR-ABL-induced oncogenesis is mediated by direct interaction with the SH2 domain of the GRB-2 adaptor protein, *Cell 75*, 175−185.
51. Orton, K. C., Ling, J., Waskiewicz, A. J., Cooper, J. A., Merrick, W. C., Korneeva, N. L., Rhoads, R. E., Sonenberg, N., and Traugh, J. A. (2004) Phosphorylation of Mnk1 by caspase-activated pak2/gamma-PAK inhibits phosphorylation and interaction of eIF4G with Mnk, *J. Biol. Chem. 279*, 38649−38657.
52. Tuazon, P. T., Spanos, W. C., Gump, E. L., Monnig, C. A., and Traugh, J. A. (1997) Determinants for substrate phosphorylation

by p21-activated protein kinase (gamma-PAK), *Biochemistry 36*, 16059−16064.
53. Smith, J. M., Katz, S., and Mayer, B. J. (1999) Activation of the Abl tyrosine kinase in vivo by Src homology 3 domains from the Src homology 2/Src homology 3 adaptor Nck, *J. Biol. Chem. 274*, 27956−27962.
54. Amoui, M., and Miller, W. T. (2000) The substrate specificity of the catalytic domain of Abl plays an important role in directing phosphorylation of the adaptor protein Crk, *Cell. Signalling 12*, 637−643.
55. Feng, S., Chen, J. K., Yu, H., Simon, J. A., and Schreiber, S. L. (1994) Two binding orientations for peptides to the Src SH3 domain: Development of a general model for SH3-ligand interactions, *Science 266*, 1241−1247.
56. Lim, W. A., Richards, F. M., and Fox, R. O. (1994) Structural determinants of peptide-binding orientation and of sequence specificity in SH3 domains, *Nature 372*, 375−379.
57. Zhou, G.-L., Zhuo, Y., King, C. C., Fryer, B. H., Bokoch, G. M., and Field, J. (2003) Akt phosphorylation of serine 21 on Pak1 modulates Nck binding and cell migration, *Mol. Cell. Biol. 23*, 8058−8069.
58. Zhao, Z.-S., Manser, E., and Lim, L. (2000) Interaction between PAK and Nck: A template for Nck targets and role of PAK autophosphorylation, *Mol. Cell. Biol. 20*, 3906−3917.
59. Ichigotani, Y., Fujii, K., Hamaguchi, M., and Matsuda, S. (2002) In search of a function for the E3B1/Abi2/Argbp1/NESH family, *Int. J. Mol. Med. 9*, 591−595.
60. Courtney, K. D., Grove, M., Vandongen, H., Vandongen, A., LaMantia, A.-S., and Pendergast, A. M. (2000) Localization and phosphorylation of Abl-interactor proteins, Abi-1 and Abi-2, in the developing nervous system, *Mol. Cell. Neurosci. 16*, 244−257.
61. Hu, H. L., Bliss, J. M., Wang, Y., and Colicelli, J. (2005) RIN1 is an ABL tyrosine kinase activator and a regulator of epithelial-cell adhesion and migration, *Curr. Biol. 15*, 815−823.
62. Rosen, M. K., Yamazaki, T., Gish, G. D., Kay, C. M., Pawson, T., and Kay, L. E. (1995) Direct demonstration of an intramolecular SH2-phosphotyrosine interaction in the Crk protein, *Nature 374*, 477−479.
63. Khwaja, A., Hallberg, B., Warne, P. H., and Downward, J. (1996) Networks of interaction of p120-cbl and p130-cas with Crk and Grb2 adaptor proteins, *Oncogene 12*, 2491−2498.
64. Okada, S., Matsuda, M., Anafi, M., Pawson, T., and Pessin, J. E. (1998) Insulin regulates the dynamic balance between Ras and Rap1 signaling by coordinating the assembly states of the Grb2-SOS and CrkII-C3G complexes, *EMBO J. 17*, 2554−2565.
65. Kain, K. H., and Klemke, R. L. (2001) Inhibition of cell migration by Abl family tyrosine kinases through uncoupling of Crk-CAS complexes, *J. Biol. Chem. 276*, 16185−16192.
66. Kain, K. H., Gooch, S., and Klemke, R. L. (2003) Cytoplasmic c-Abl provides a molecular 'rheostat' controlling carcinoma cell survival and invasion, *Oncogene 22*, 6071−6080.

BI701533J